

BLACK HOLES

A noninteracting low-mass black hole–giant star binary system

Todd A. Thompson^{1,2,3*}, Christopher S. Kochanek^{1,2}, Krzysztof Z. Stanek^{1,2}, Carles Badenes^{4,5}, Richard S. Post⁶, Tharindu Jayasinghe^{1,2}, David W. Latham⁷, Allyson Bieryla⁷, Gilbert A. Esquerdo⁷, Perry Berlind⁷, Michael L. Calkins⁷, Jamie Tayar^{1,8}, Lennart Lindegren⁹, Jennifer A. Johnson^{1,2}, Thomas W.-S. Holien¹⁰, Katie Auchettl^{2,11,12}, Kevin Covey¹³

Black hole binary systems with companion stars are typically found via their x-ray emission, generated by interaction and accretion. Noninteracting binaries are expected to be plentiful in the Galaxy but must be observed using other methods. We combine radial velocity and photometric variability data to show that the bright, rapidly rotating giant star 2MASS J05215658+4359220 is in a binary system with a massive unseen companion. The system has an orbital period of ~83 days and near-zero eccentricity. The photometric variability period of the giant is consistent with the orbital period, indicating star spots and tidal synchronization. Constraints on the giant's mass and radius imply that the unseen companion is $3.3^{+2.8}_{-0.7}$ solar masses, indicating that it is a noninteracting low-mass black hole or an unexpectedly massive neutron star.

The observed distributions of neutron star and stellar black hole masses are connected to the mechanism of core-collapse supernovae, its rate as the Universe evolves, and the physics of binary stars (1, 2). An unbiased census of neutron star and black hole masses is required to understand these interconnected areas. However, our knowledge of neutron star and black hole demography is limited because mass measurements are obtained almost exclusively for pulsar and accreting binary systems selected from radio, x-ray, and gamma-ray surveys (3–5). While gravitational microlensing has the potential to reveal compact object mass distributions (6), individual systems are difficult to characterize. The detections of merging black hole and neutron star binaries by gravitational wave experiments (7, 8) provide compact object masses, but these merging systems are an intrinsically biased subset of the parent population.

Studies of compact object populations are complemented by those of massive star binary systems (9), whose more massive “primary” components ultimately produce neutron stars and black holes [for stars $>10 M_{\odot}$ (solar masses)]. These studies reveal a broad distribution of secondary masses and orbital periods, implying that many massive stars have low-mass, long-lived companions. Quiescent noninteracting black hole stellar binaries have not been found in radial velocity searches, although the existence of such systems has been discussed for decades (10, 11). The only known candidate formed by dynamical scattering processes in a dense globular cluster (12), so it did not form as an isolated binary in the more typical Galactic field environment. Although subject to their own selection biases, a sample of Galactic binary star systems with black hole or neutron star companions would inform binary evolution models, which are currently limited by comparison to pulsar binaries and interacting or merging systems.

We searched for stellar binaries with massive unseen companions in data from the Apache Point Observatory Galactic Evolution Experiment (APOGEE) (13). APOGEE provides multi-epoch near-infrared spectroscopy for $>10^5$ stars in the Milky Way. These observations provide stellar elemental abundances and can also reveal radial velocity variations indicative of binary orbital motion (14). We searched for systems with large apparent accelerations—the difference in radial velocity divided by the difference in time between two epochs. Systems were ranked by an estimate of the binary mass function given the irregular timing of the APOGEE observation epochs.

Although the radial velocity measurements from APOGEE can immediately indicate the presence of a binary, the mass of the companion is not determined, because the orbital period, inclination, and eccentricity are unknown.

To constrain the orbital periods of the ~200 APOGEE sources with the highest accelerations, we searched for periodic variations in photometric data from the All-Sky Automated Survey for Supernovae (ASAS-SN) (15, 16) for evidence of transits, ellipsoidal variations, or star spots. This process identified the giant star 2MASS J05215658+4359220 (hereafter J05215658), which exhibits an acceleration of $\approx 2.9 \text{ km s}^{-1} \text{ day}^{-1}$ and periodic photometric variability with a period of $\approx 82.2 \pm 2.5$ days (Fig. 1 and table S2). This system lies in the constellation Auriga, near the outer Galactic plane, with Galactic coordinates $(l, b) = (164.774^\circ, 4.184^\circ)$.

Previous analysis of J05215658 determined an effective stellar temperature $T_{\text{eff}} \approx 4480 \pm 62 \text{ K}$, a surface gravitational acceleration $\log [g/(\text{cm s}^{-2})] \approx 2.59 \pm 0.06$, and a near-Solar value for the carbon-to-nitrogen abundance ratio (17). Our analysis of the APOGEE spectrum yields a projected rotational velocity of $v \cdot \sin i_{\text{rot}} \approx 14.1 \pm 0.6 \text{ km s}^{-1}$ (18), where i_{rot} is the inclination angle of the rotation axis projected onto the plane of the sky. We obtained additional optical spectra with the Tillinghast Reflector Echelle Spectrograph (TRES), which indicate a consistent effective temperature but lower $\log g \approx 2.35 \pm 0.14$, and higher $v \cdot \sin i_{\text{rot}} \approx 16.8 \pm 0.6 \text{ km s}^{-1}$. We adopt the TRES $\log g$ and the APOGEE $v \cdot \sin i_{\text{rot}}$ in our analysis (18).

We further constrained the system using radial velocity and multiband photometric follow-up (Fig. 2). The photometric variability amplitude increases from the redder to bluer bands. The shape, character, and phasing of the light curve are inconsistent with stellar pulsations or ellipsoidal variations but are typical of the class of spotted K-type giants such as HD 1833, V1192 Orionis, and KU Pegasi (19, 20). Binary systems with periods less than ~150 days often have low eccentricities, implying rapid tidal circularization (21, 22). The change in the shape of the light curve over time (Fig. 1) is likely due to star spot evolution.

Figure 2B shows the TRES radial velocity measurements. The APOGEE and TRES spectra exhibit only a single set of absorption lines, i.e., a single-lined spectroscopic binary. The system has a nearly circular orbit with orbital period $P_{\text{orb}} \approx 83.2 \pm 0.06$ days, radial velocity semi-amplitude $K \approx 44.6 \pm 0.1 \text{ km s}^{-1}$, and eccentricity $e \approx 0.0048 \pm 0.0026$. The mass function is

$$f(M) \equiv \frac{M_{\text{CO}}^3 \sin^3 i_{\text{orb}}}{(M_{\text{giant}} + M_{\text{CO}})^2} = \frac{K^3 P_{\text{orb}}}{2\pi G} (1 - e^2)^{3/2} \approx 0.766 \pm 0.006 M_{\odot} \quad (1)$$

where G is the gravitational constant, M_{CO} is the compact object companion mass, i_{orb} is the orbital inclination, and M_{\odot} is the mass of the Sun. Figure 3 shows allowed values of M_{CO} as a function of the mass of the giant star M_{giant}

¹Department of Astronomy, The Ohio State University, 140 W. 18th Ave., Columbus, OH 43210, USA. ²Center for Cosmology and AstroParticle Physics, The Ohio State University, 191 W. Woodruff Ave., Columbus, OH 43210, USA. ³Institute for Advanced Study, 1 Einstein Dr., Princeton, NJ 08540, USA. ⁴Department of Physics and Astronomy and Pittsburgh Particle Physics, Astrophysics and Cosmology Center, University of Pittsburgh, 3941 O'Hara St., Pittsburgh, PA 15260, USA. ⁵Institut de Ciències del Cosmos, Universitat de Barcelona, Martí Franqués 1, E08028 Barcelona, Spain. ⁶Post Observatory, Lexington, MA 02421, USA. ⁷Harvard-Smithsonian Center for Astrophysics, 60 Garden St., Cambridge, MA 02138, USA. ⁸Institute for Astronomy, University of Hawaii, 2680 Woodlawn Dr., Honolulu, Hawaii 96822, USA. ⁹Lund Observatory, Department of Astronomy and Theoretical Physics, Lund University, Box 43, 22100 Lund, Sweden. ¹⁰The Observatories of the Carnegie Institution for Science, 813 Santa Barbara St., Pasadena, CA 91101, USA. ¹¹Department of Physics, The Ohio State University, 191 W. Woodruff Ave., Columbus, OH 43210, USA. ¹²Dark Cosmology Centre, Niels Bohr Institute, University of Copenhagen, Lyngbyvej 2, 2100 Copenhagen, Denmark. ¹³Department of Physics and Astronomy, Western Washington University, Mail Stop 9164, Bellingham, WA, 98225, USA.

*Corresponding author. Email: thompson.1847@osu.edu

for several values of $\sin i_{\text{orb}}$. For $M_{\text{giant}} \geq 1 M_{\odot}$ and $\sin i_{\text{orb}} = 1.0$, the minimum possible companion mass is $M_{\text{CO}} \geq 1.8 M_{\odot}$. The observed spectral energy distribution (SED) is inconsistent with a stellar companion of such high mass (18) (fig. S8). We conclude that the unseen companion is either a massive neutron star or a black hole. Follow-up x-ray observations yield a tight upper limit on emission from the system (18).

To determine the nature of the compact object companion we must constrain the mass of the giant and the orbital inclination. We can estimate minimum values of the giant radius and bolometric luminosity using the star's projected rotation velocity. The low orbital eccentricity and the correspondence between the orbital and photometric periods imply that the system is tidally circularized and synchronized. We therefore adopt the hypothesis that the giant's rotational period is equal to the binary orbital period and that they have the same inclination ($i_{\text{rot}} = i_{\text{orb}} = i$). This yields a minimum radius of $R \simeq 23 \pm 1 R_{\odot}/\sin i$, a minimum luminosity $L = 4\pi R^2 \sigma_{\text{SB}} T_{\text{eff}}^4 \simeq 210 \pm 20 L_{\odot}/\sin^2 i$ for $T_{\text{eff}} \simeq 4500$ K, and a minimum distance $D \simeq [L/(4\pi F)]^{1/2} \simeq 2.45 \pm 0.1$ kpc/ $\sin i$, where R_{\odot} is the radius of the Sun, L_{\odot} is the luminosity of the Sun, σ_{SB} is the Stefan-Boltzmann constant, and F is the bolometric (all-wavelength) flux measured from the SED (18). Combining the minimum giant radius with the TRES $\log g \simeq 2.35 \pm 0.14$ gives an estimate for the giant mass of $M_{\text{giant}}^{\log g} = gR^2/G \simeq 4.4^{+2.2}_{-1.5} M_{\odot}/\sin^2 i$, implying a minimum companion mass of $M_{\text{CO}} \gtrsim 2.9 M_{\odot}$.

Alternatively, R and L can be determined directly from the measured distance and flux. The parallax of this system measured by the Gaia satellite is 0.272 ± 0.049 milliarcseconds (mas) (23), corresponding to a nominal distance of 3.7 kpc, but there are systematic offsets in the Gaia parallaxes that are a function of both sky position and brightness (23). Additionally, the companion will induce astrometric binary motion of the giant that is not accounted for in Gaia's parallax measurement (23). Given $f(M)$ and P , the ratio of the binary angular motion to the parallax is $0.34/\sin i$, which could bias the measured parallax. Applying a zero-point offset and an additional systematic uncertainty, and accounting for the phased binary motion with the geometry and timing of the observations by Gaia for J05215658 using Monte Carlo simulations for an arbitrary orbital sky projection (18), we find a parallax of $\pi \simeq 0.322^{+0.086}_{-0.074}$ mas (1σ confidence interval) for all $\sin i > 0$, corresponding to a distance $D \simeq 3.11^{+0.93}_{-0.66}$ kpc. The observed flux then gives $L \simeq 331^{+231}_{-127} L_{\odot}$ and $R \simeq 30^{+9}_{-6} R_{\odot}$, consistent with the estimates from $v \cdot \sin i$. Combining the Gaia lower bound of $R \simeq 24 R_{\odot}$ with the TRES $\log g$ gives $M_{\text{giant}}^{\log g} \gtrsim 4.8 M_{\odot}$ and a value of M_{CO} in the black hole regime (Fig. 3).

Direct comparison between $R \simeq 30^{+9}_{-6}$ derived from the parallax and $R \simeq 23 \pm 1 R_{\odot}/\sin i$ derived from $v \cdot \sin i$ suggests that $\sin i \simeq 0.8 \pm 0.2$. The 2σ upper limit on the Gaia parallax of 0.486 mas for $\sin i > 0.6$, gives lower limits of $L \gtrsim 150 L_{\odot}$ and $R \gtrsim 20 R_{\odot}$ (18). The TRES $\log g = 2.35 \pm 0.14$ then gives $M_{\text{giant}}^{\log g} \gtrsim 3.2^{+1.2}_{-0.9} M_{\odot}$,

implying a lower limit on the companion mass of $M_{\text{CO}} \gtrsim 2.5 M_{\odot}$.

The giant mass can also be estimated by comparing its properties to single-star evolutionary models, with the caveats that (i) strong binary interaction likely occurred in the history of the system, and (ii) rapidly rotating, spotted

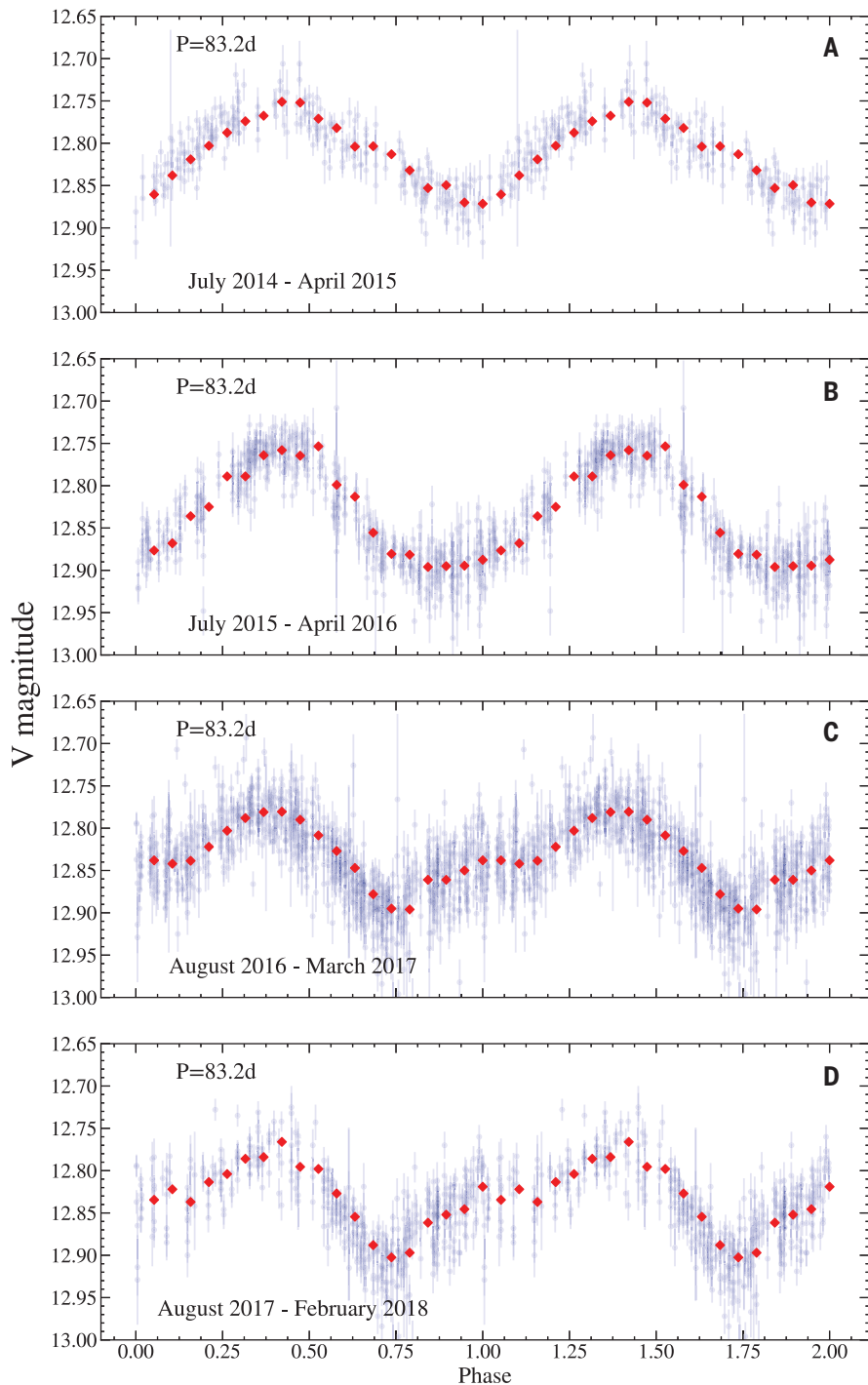


Fig. 1. Multi-epoch ASAS-SN light curves. V-band ASAS-SN light curves for J05215658 over four observing seasons (**A** to **D**), phased to the orbital period of 83.2 days and duplicated over two periods. Blue points are the observed data with 1σ error bars. Red points are the running median of 20 data points. The same data before phasing are shown in fig. S1.

Fig. 2. Multicolor light curves and TRES radial velocities. (A) The *B*-band (lowest, triangles), *V*-band (pentagons), *r*-band (circles), and *i*-band (highest, squares) light curves with arbitrary zero-point offsets applied for display. (B) The TRES radial velocity (RV) measurements as a function of heliocentric Julian date (HJD). Maximum blueshift (negative RV) occurs near the photometric maximum in all bands, and maximum redshift occurs after photometric minimum, near the shoulder or plateau in the light curve at HJD – 2,450,000 ≈ 8080. Figure 1 shows the evolution of the phased multi-epoch *V*-band ASAS-SN light curve for comparison.

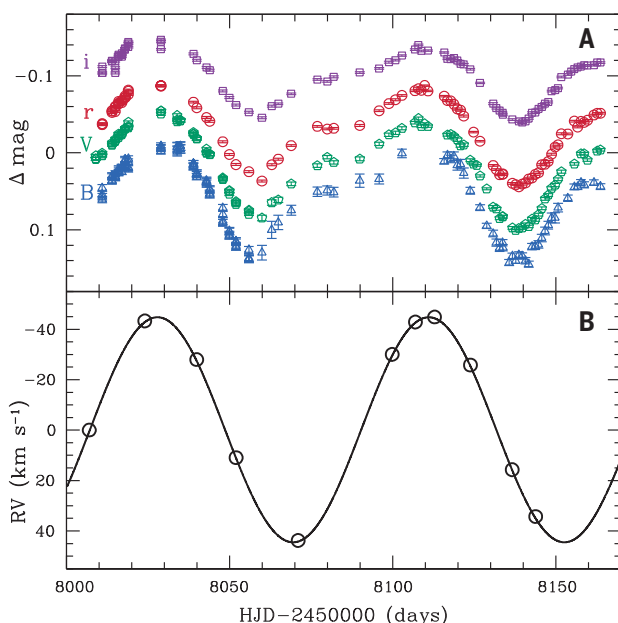
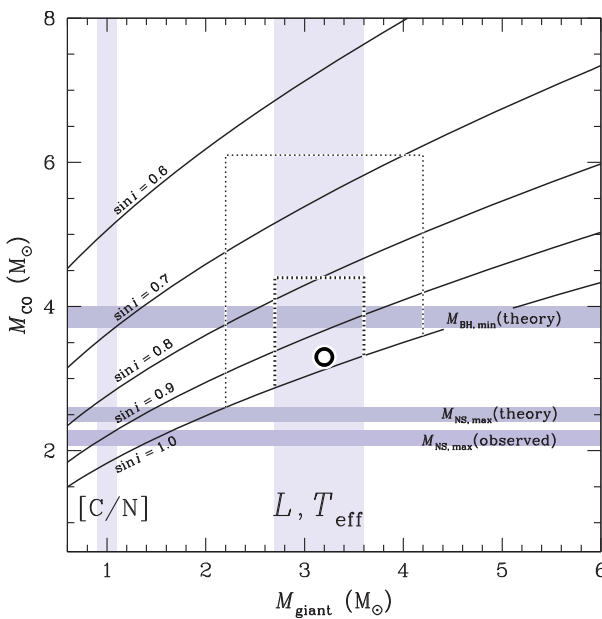


Fig. 3. Compact object mass constraints. Solutions to the mass function (solid black lines) for the compact object's mass M_{CO} as a function of the giant's mass M_{giant} at five values of the orbital inclination from $\sin i = 1.0$ to 0.6. The vertical band labeled L, T_{eff} denotes the best-fitting range of M_{giant} when the giant's measured L, T_{eff} , and $\log g$ are matched to theoretical single-star evolutionary models. The regions enclosed by the thick and thin dashed lines show the resulting 1σ and 2σ mass ranges, respectively. The best-fitting value is denoted with the empty circle. The vertical band labeled [C/N] denotes the range of M_{giant} implied by the observed carbon to nitrogen ratio and the mean locus of the observed [C/N] – M_{giant} correlation for giant stars (18), although we regard this solution as unlikely (see text). The horizontal bands denote the largest observed neutron star mass (lowest), a theoretical maximum neutron star mass (middle), and a theoretical minimum black hole mass (top).



giants like J05215658 are observed to be redder than expected for a given luminosity, underestimating the true dynamical mass (24). Nevertheless, we searched for the best-fitting model over a range of stellar metallicity and with the constraint $\log g = 2.35 \pm 0.14$, and the other parameters (L, R , and T_{eff}) inferred from the parallax and SED. We found it difficult to simultaneously match the temperature and surface gravity, which is a known systematic problem for models of giant stars (25). The

best matches were for solar metallicity models. Combining all models, the joint best-fitting mass is $M_{\text{giant}} \approx 3.2^{+1.0}_{-1.0} M_{\odot}$ (2σ), shown in Fig. 3. The model fitting is driven to a giant mass of 2 to $4 M_{\odot}$ primarily by the L and R inferred from the parallax and SED. Given the APOGEE measurement of $v \cdot \sin i$, the best-fitting mass implies $\sin i \approx 0.97^{+0.03}_{-0.12}$. Solving the mass function $f(M)$ for this range of M_{giant} and $\sin i$ yields $M_{\text{CO}} \approx 3.3^{+2.8}_{-0.7} M_{\odot}$ (2σ ; also shown in Fig. 3). While a lower assumed value of $v \cdot \sin i$

allows for a lower mass giant, it also leads to a smaller $\sin i$ that drives M_{CO} upwards. Similarly, if we assume a lower $\log g$, or impose no constraint on $\log g$, we obtain best-fitting giant masses at the low end of the range denoted in Fig. 3 ($M_{\text{giant}} \approx 2.2$ – $2.5 M_{\odot}$), but with compact object companion masses of ≈ 2.9 to $4.0 M_{\odot}$.

All of our determinations consistently require $M_{\text{giant}} \sim 2$ to $4 M_{\odot}$. Stars in this mass range are rare in APOGEE (18). However, J05215658 would be unusual even among APOGEE's massive giants because it has a near-solar carbon-to-nitrogen abundance ratio. Giants exhibit a strong correlation between this abundance ratio and mass that would imply a low value of $M_{\text{giant}} \approx 1.0 M_{\odot}$ for J05215658. We also show this "low-mass giant" possibility in Fig. 3 but consider it highly unlikely, because it is inconsistent with the mass determination from all other methods, and because some higher-mass giants with solar carbon-to-nitrogen abundance ratios do exist in the APOGEE sample (18).

We conclude that J05215658 likely consists of a $\approx 3.2^{+1.0}_{-1.0} M_{\odot}$ giant star and a noninteracting low-mass black hole companion with $M_{\text{CO}} \approx 3.3^{+2.8}_{-0.7} M_{\odot}$ (the 2σ range in Fig. 3). This range of compact object mass falls in the so-called mass gap between neutron stars and black holes (5). It is above the highest neutron star masses thus far observed [$2.01 \pm 0.04 M_{\odot}$ (26) and $2.14^{+0.10}_{-0.09} M_{\odot}$ (27)], and the uncertainty range nearly spans from the predicted theoretical maximum neutron star mass [$\approx 2.5 M_{\odot}$ (28)] to the lowest well-measured black hole masses [5 to $6 M_{\odot}$ (4, 5)]. Whereas some models of black hole formation indicate a lower mass limit of $\sim 4 M_{\odot}$ (1, 29), others predict a wide range of masses throughout the mass gap (30, 31). J05215658 joins a handful of other known binaries that may host compact objects in this mass range, including the x-ray binaries GX 339-4 [2.3 to $9.5 M_{\odot}$ (32)] and 4U 1543-47 [2.7 to $7.5 M_{\odot}$ (33)].

REFERENCES AND NOTES

1. O. Pejcha, T. A. Thompson, *Astrophys. J.* **801**, 90 (2015).
2. K. Belczynski, V. Kalogera, T. Bulik, *Astrophys. J.* **572**, 407–431 (2002).
3. F. Özel, D. Psaltis, R. Narayan, A. Santos Villarreal, *Astrophys. J.* **757**, 55 (2012).
4. F. Özel, D. Psaltis, R. Narayan, J. E. McClintock, *Astrophys. J.* **725**, 1918–1927 (2010).
5. W. M. Farr et al., *Astrophys. J.* **741**, 103 (2011).
6. B. Paczynski, *Astrophys. J.* **304**, 1 (1986).
7. LIGO Scientific Collaboration and Virgo Collaboration, *Phys. Rev. Lett.* **116**, 061102 (2016).
8. LIGO Scientific Collaboration and Virgo Collaboration, *Phys. Rev. Lett.* **119**, 161101 (2017).
9. H. A. Kobulnicky et al., *Astrophys. J.* **213** (suppl.), 34 (2014).
10. O. K. Guseinov, Y. B. Zel'dovich, *Sov. Astron.* **10**, 251 (1966).
11. V. L. Trimble, K. S. Thorne, *Astrophys. J.* **156**, 1013 (1969).
12. B. Giesers et al., *Mon. Not. R. Astron. Soc.* **475**, L15–L19 (2018).
13. S. R. Majewski et al., *Astrophys. J.* **154**, 94 (2017).
14. C. Badenes et al., *Astrophys. J.* **854**, 147 (2018).
15. B. J. Shappee et al., *Astrophys. J.* **788**, 48 (2014).
16. C. S. Kochanek et al., *Publ. Astron. Soc. Pac.* **129**, 104502 (2017).

17. B. Abolfathi *et al.*, *Astrophys. J.* **235** (suppl.), 42 (2018).
18. Additional data, materials, and methods are provided as supplementary materials.
19. K. G. Strassmeier, L. Kratzwald, M. Weber, *Astron. Astrophys.* **408**, 1103–1113 (2003).
20. M. Weber, K. G. Strassmeier, *Astron. Astrophys.* **373**, 974–986 (2001).
21. M. Mayor, J. C. Mermilliod, in *Observational Tests of the Stellar Evolution Theory*, A. Maeder, A. Renzini, Eds., vol. 105 of *International Astronomical Union Symposia* (Springer, 1984), p. 411.
22. F. Verbunt, E. S. Phinney, *Astron. Astrophys.* **296**, 709 (1995).
23. L. Lindegren *et al.*, *Astron. Astrophys.* **616**, A2 (2018).
24. K. Oláh *et al.*, *Astron. Astrophys.* **620**, A189 (2018).
25. J. Tayar *et al.*, *Astrophys. J.* **807**, 82 (2015).
26. J. Antoniadis *et al.*, *Science* **340**, 1233232 (2013).
27. H. T. Cromartie *et al.*, *Nat. Astron.* 10.1038/s41550-019-0880-2 (2019).
28. J. M. Lattimer, *Annu. Rev. Nucl. Part. Sci.* **62**, 485–515 (2012).
29. C. S. Kochanek, *Astrophys. J.* **785**, 28 (2014).
30. S. E. Woosley, T. A. Weaver, *Astrophys. J.* **101** (suppl.), 181 (1995).
31. D. Kushnir, Thermonuclear explosion of rotating massive stars could explain core-collapse supernovae. arXiv:1502.03111 [astro-ph.HE] (10 February 2015).
32. M. Heida, P. G. Jonker, M. A. P. Torres, A. Chiavassa, *Astrophys. J.* **846**, 132 (2017).
33. J. A. Orosz, R. K. Jain, C. D. Bailyn, J. E. McClintock, R. A. Remillard, *Astrophys. J.* **499**, 375–384 (1998).

ACKNOWLEDGMENTS

We thank J. Choi for making MIST models available and C. Jordi and C. Fabricius for discussions. We thank the Ohio State University College of Arts and Sciences Technology Services for setting up the ASAS-SN Sky Patrol light curve server, which was critically useful during this work. T.A.T. thanks J. Zinn, T. Sukhbold, S. Gaudi, O. Pejcha, K. Stassun, M. Pinsonneault, A. Brown, C. Gammie, E. Rossi, J. Fuller, S. Phinney, A.-C. Elters, D. Hogg, K. Cunha, and R. Poleski for discussions, and K. A. Byram for encouragement and support. Full facility acknowledgments are provided in the supplementary materials. **Funding:** T.A.T. acknowledges support from Scialog Scholar grant 24216 from the Research Corporation; a Simons Foundation Fellowship; and an IBM Einstein Fellowship from the Institute for Advanced Study, Princeton. C.B. acknowledges support from PHY 14-30152: Physics Frontier Center/JINA Center for the Evolution of the Elements (JINA-CEE), awarded by the National Science Foundation. C.S.K. and K.Z.S. are supported in part by NSF grants AST-1515927 and AST-1515876. J.T. acknowledges support from NASA Hubble Fellowship grant 51424 awarded by the Space Telescope Science Institute, which is operated by the Association of Universities for Research in Astronomy, Inc., for NASA, under contract NAS5-26555. **Author contributions:** T.A.T. led the project, conceived of the search strategy, led the analysis, and led the writing of the text. C.S.K. analyzed the SED and the ASAS-SN photometry and fitted the observational data with evolutionary models. K.Z.S. analyzed the Post and ASAS-SN photometry and interpreted the system. R.S.P. provided the Post photometry. C.B. provided APOGEE RV analysis and interpretation of the system. T.J. carried out the

time-series analysis of the ASAS-SN photometry. D.W.L., A.B., G.A.E., P.B., and M.L.C. obtained the TRES data and carried out the RV analysis. J.T. provided the rotation measurement from the APOGEE spectrum. LL. provided the Gaia parallax bias analysis. J.A.J. consulted on the APOGEE spectra. T.W.-S.H. and K.A. obtained and analyzed the Swift data. K.C. participated in preparing the text and discussions of the APOGEE RV data. **Competing interests:** There are no competing interests to declare. **Data and materials availability:** The ASAS-SN light curve data are available at <https://asas-sn.osu.edu/photometry/166c0fc-2502-5e10-b5aa-38d31dddb398>. The APOGEE observations, including all individual spectra, the combined spectrum, and analysis results are available at <https://dr14.sdss.org/infrared/spectrum/view/stars?id=68401>. Photometry for J05215658 is listed in table S8. X-ray and ultraviolet observations from the Neil Gehrels Swift Observatory (*J8*) are available at <https://heasarc.gsfc.nasa.gov/cgi-bin/W3Browse/swift.pl> under target id 10442. The code used to calculate the parallax bias in the Gaia observations is available at https://github.com/chargedcurrent/Gaia_parallax_J05215658.

SUPPLEMENTARY MATERIALS

science.sciencemag.org/content/366/6465/637/suppl/DC1
Materials and Methods
Figs. S1 to S9
Tables S1 to S8
References (34–89)

7 June 2018; accepted 10 October 2019
10.1126/science.aau4005

A noninteracting low-mass black hole–giant star binary system

Todd A. Thompson¹ Christopher S. Kochanek² Krzysztof Z. Stanek³ Carles Badenes⁴ Richard S. Post⁵ Tharindu Jayasinghe⁶ David W. Latham⁷ Allyson Bieryla⁸ Gilbert A. Esquerdo⁹ Perry Berlind¹⁰ Michael L. Calkins¹¹ Jamie Tayar¹² Lennart Lindegren¹³ Jennifer A. Johnson¹⁴ Thomas W.-S. Holoi¹⁵ Katie Auchettl¹⁶ Kevin Covey¹⁷

Science, 366 (6465), • DOI: 10.1126/science.aau4005

A black hole hiding in a binary star

As material falls toward a black hole, it heats up and emits x-rays. Almost all black holes are discovered by this x-ray emission. Thompson *et al.* observed light from a giant star that is Doppler shifted, indicating an orbit around a binary companion. The companion object must weigh more than 2.6 solar masses, but it emits no light, including x-rays. This indicates the presence of a black hole that is not currently consuming any material. There may be a population of similarly hidden black holes that have been missed by x-ray observations.

Science, this issue p. 637

View the article online

<https://www.science.org/doi/10.1126/science.aau4005>

Permissions

<https://www.science.org/help/reprints-and-permissions>